Stress Analysis of Axisymmetric Solids with Asymmetric Properties

JAMES G. CROSE*
The Aerospace Corporation, San Bernardino, Calif.

The finite element method for the determination of stresses and displacements in arbitrary axisymmetric solids is extended to problems involving asymmetric mechanical and thermal loads and materials with asymmetric temperature dependent mechanical properties. All dependent variables, including the mechanical properties, are represented by a Fourier series expansion of the circumferential coordinate. Due to the mechanical property variation in the circumferential direction, the resulting equation set becomes fully coupled and must be solved simultaneously. By grouping all Fourier coefficients together at each nodal point, a banded stiffness matrix is achieved the efficient solution of which is feasible by the use of a blocked square root Cholesky method. A user-oriented computer program based on the method of analysis is described and applied to several example problems to verify accuracy and demonstrate versatility of the program.

Introduction

THE finite element method of stress analysis of axisymmetric solids subjected to axisymmetric or nonaxisymmetric loads was initially formulated by Wilson.[1] This work has formed the basis for the development of many highly sophisticated computer programs[2-4] that have proved to be of great value to structural analysts. In the aerospace industry, typical problems requiring the generality of these methods include thermal stress analysis of re-entry vehicle nosetips and heatshields, rocket nozzles and cases, solid propellant grains, spacecraft heatshields, boosters, etc. The present state-of-the-art of these methods of analysis is restricted to axisymmetric bodies loaded by symmetric[2,3] or nonsymmetric[4] mechanical loads,[4] thermal stresses,[2,3] or internal pore pressures.[2] A considerably more general class of problems involves axisymmetric bodies composed of materials which have nonsymmetric properties. This type of problem arises frequently in thermal stress analyses because material properties are in general dependent upon temperature. That is, for an asymmetric temperature field, the mechanical properties become asymmetric. This article presents a method of thermal stress analysis that is directly applicable to problems of axisymmetric structures with circumferentially varying material properties. Although this class of problems can be solved in an alternative way by use of three-dimensional finite element methods,[5] the method presented herein promises to be much more efficient.

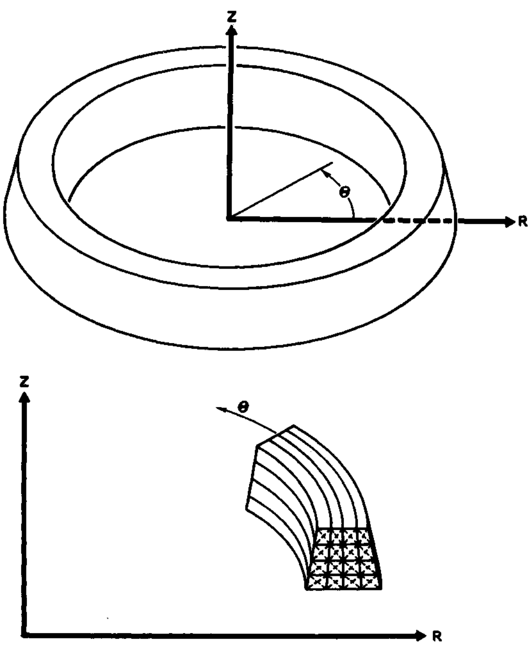

Fig. 1 Finite element idealization.

Method of Analysis

The method of analysis employed herein is based on a finite element idealization of an axisymmetric solid. Each element is an axisymmetric ring of triangular cross section. Since such a solid may be loaded and may deform in nonaxisymmetric modes and since the properties of the material may vary in all directions (e.g., due to temperature variations), all the dependent variables including the material properties are expressed as truncated Fourier series with the circumferential coordinate being the independent variable.

Figure 1 illustrates the idealization of a typical axisymmetric solid and defines the cylindrical coordinate system. It is noted in Fig. 1 that the solid lines denote a system of quadrilateral elements. Within the computer program based on this method, quadrilateral elements are subdivided into four triangular elements for formulation of stiffnesses, loads, etc. Then, the center point is eliminated yielding a formulation based on an arbitrary quadrilateral mesh. The advantage of this operation is to reduce the number of equations needed for solution of the problem and to allow the use of certain automatic mesh generation procedures.

The advantage of the method described herein is that material properties may vary in all three directions within the solid. This enables the method to be applied to thermal stress analysis problems in which the material properties are temperature dependent and temperatures vary circumferentially. Similar approaches[1,4] have been taken in the past but all have required that the varying material properties do not vary circumferentially. The essential feature of those methods was that the orthogonality condition could be used to uncouple the Fourier series. In the present method, harmonics are coupled and all equations must be solved simultaneously. Due to the appropriate arrangement of

Received July 26, 1971; revision received February 11, 1972.
Index categories: Thermal Stresses; Structural Static Analysis.
* Member of the Technical Staff.

equations,[6] the method is feasible for application on the present generation of computers.

Equilibrium Equations

Equilibrium equations of a finite element system have been previously derived.[1-4] By assuming a linear displacement field in each triangular element, applying the strain displacement relationship and Hooke's law, the strain energy may be formulated. After summing the contributions of all elements and minimizing the total potential energy of the entire assemblage, the result is a system of simultaneous linear algebraic equations,

$$\sum_{n=1}^{N}\left[\int_{\text{Vol.}}[a^n]^T[C^n][a^n]\,dV\right]\{u\} = \sum_{n=1}^{N}\left[\int_{\text{Vol.}}[a^n]^T\{\tau^n\}\,dV\right] + \sum_{n=1}^{N}\left[\int_{\text{Vol.}}[d^n]^T\{F^n\}\,dV\right] + \sum_{n=1}^{N}\left[\int_{\text{Area}}[d^n]^T\{P^n\}\,dA\right] \quad (1)$$

where for the nth element, $[a^n]$ is the functional relationship between nodal point displacement and element strain, $[C^n]$ is the relationship between stress and strain, $\{u\}$ is the vector of unknown nodal point displacements, $\{\tau^n\}$ is the vector of thermal stresses, $\{F^n\}$ is the vector of element body forces transformed to nodal point values, and $\{P^n\}$ is the vector of surface tractions.

All of the dependent variables including $[C^n]$ are expressed in the form of a Fourier series to account for circumferential variations. Therefore, integrations on the left-hand side of Eq. (1) involve a triple product of trigonometric terms and integrations on the right-hand side involve a simple product of two trigonometric terms. This results in full coupling of displacement harmonics with load harmonics.

Element Stiffness Matrix

Derivation of the element stiffness matrix requires that the dependent variables and material properties be expanded in the form of a Fourier series. The strain displacement relations are

$$\varepsilon_{rr} = \partial w_r/\partial r \quad (2a)$$

$$\varepsilon_{zz} = \partial w_z/\partial z \quad (2b)$$

$$\varepsilon_{\theta\theta} = 1/r[(\partial w_\theta/\partial\theta) + w_r] \quad (2c)$$

$$\varepsilon_{rz} = \partial w_r/\partial z + \partial w_z/\partial r \quad (2d)$$

$$\varepsilon_{r\theta} = 1/r[(\partial w_r/\partial\theta) - w_\theta] + \partial w_\theta/\partial r \quad (2e)$$

$$\varepsilon_{z\theta} = \partial w_\theta/\partial z + (1/r)\,\partial w_z/\partial\theta \quad (2f)$$

In what follows, the superscript n which denoted a typical element in the previous section will be omitted for convenience. The displacements within an element are assumed to be in the following form:

$$w_r = \sum_{m=0}^{M}(b_{1m} + rb_{2m} + zb_{3m})\cos m\theta \quad (3a)$$

$$w_z = \sum_{m=0}^{M}(b_{4m} + rb_{5m} + zb_{6m})\cos m\theta \quad (3b)$$

$$w_\theta = \sum_{m=0}^{M}(b_{7m} + rb_{8m} + zb_{9m})\sin m\theta \quad (3c)$$

Note that a plane of symmetry has been introduced by neglecting part of the Fourier series. This was done to simplify the presentation of the method. Extension to the complete Fourier series form is tedious, but simple in concept.

By combining Eqs. (2a–f) and (3a–c) and performing the differentiations,

$$\{\varepsilon\} = \sum_{m=0}^{M}[\theta_m][g_m][b_m] \quad (4)$$

The individual matrices in Eq. (4) are given in the appendix.

The coefficients b may be found by evaluating Eq. (3a–c) at the vertices i, j, k of the triangular element. For each harmonic

$$\{b_m\} = [h]\{u_m\} \quad (5)$$

where $[h]$ is a function of the nodal point coordinates and is given in the appendix.

Therefore, the element strain can be written as a function of nodal point displacements

$$\{\varepsilon\} = \sum_{m=0}^{M}[\theta_m][g_m][h]\{u_m\} \quad (6)$$

Hence, the expression for $[a]$ in Eq. (1) has been derived. It is:

$$[a] = \sum_{m=0}^{M}[\theta_m][g_m][h] \quad (7)$$

In the remainder of the element stiffness derivation, it will be necessary to distinguish between "displacement," "load," and "material" harmonics with the sub and subsubscripts d, l, and m.

The material properties are assumed to be representable by a Fourier series of the following form

$$[C] = \sum_{m_m=0}^{M_m}[C_{m_m}]\cos m_m\theta \quad (8)$$

where the individual matrices are given in the appendix. The element stiffness may now be formed. It can be shown that $[a]^T$ refers to "load" harmonics. Therefore,

$$[k] = \sum_{m_l=0}^{M_l}\sum_{m_d=0}^{M_d}[h]^T\left[\int_{\text{Vol.}}\sum_{m_m=0}^{M_m}[g_{m_l}]^T[\theta_{m_l}]^T \times \cos m_m\theta[C_{m_m}][\theta_{m_d}][g_{m_d}]\,dV\right][h] \quad (9)$$

The element stiffness matrix can also be written as the double sum

$$[k] = \sum_{m_l=0}^{M_l}\sum_{m_d=0}^{M_d}[h]^T[\phi_{m_l,m_d}][h] \quad (10)$$

where the matrix $[\phi_{m_l,m_d}]$ has been derived by performing the summation and multiplications implied in Eq. (9) and is given in the appendix. For every term in $[\phi_{m_l,m_d}]$ integration in the θ direction consists of evaluating the integral of a triple product of sine and/or cosine functions. This gives rise to a special rule for combining material property harmonics in each term of $[\phi_{m_l,m_d}]$ which is described in the appendix. The matrix $[\phi_{m_l,m_d}]$ is assembled directly in the associated computer program.

Element Load Vector

The element load vector consists of body forces $\{F\}$, thermal stresses $\{\tau\}$ and surface tractions $\{P\}$. The body forces and surface tractions are idealized directly with a Fourier series representation. However, the thermal stress is a function of the material properties, the coefficient of thermal expansion, and the temperature of the element. In general, each of these quantities can be expressed as an independent Fourier series. Therefore,

$$\{\tau\} = \sum_{m_1=0}^{M_1}\sum_{m_2=0}^{M_2}\sum_{m_3=0}^{M_3}T_{m_1}[C_{m_2}]\{\alpha_{m_3}\}\cos m_1\theta\cos m_2\theta\cos m_3\theta \quad (11)$$

In order to be compatible with the form of the other components of the load vector, Eq. (11) is converted to the following Fourier series form:

$$\{\tau\} = \sum_{m_l=0}^{M_l}\{\tau_{m_l}\}\cos m_l\theta \quad (12)$$

where for each harmonic, the individual terms of $\{\tau_{m_l}\}$ are found by inspection to be

$$\{\tau_{m_l}\} = \frac{1}{4}\sum_{m_1=0}^{M_1}\sum_{m_2=0}^{M_2}\sum_{m_3=0}^{M_3}(\beta_1+\beta_2+\beta_3+\beta_4)T_{m_1}[C_{m_2}]\{\alpha_{m_3}\} \quad (13)$$

and where the following special rule is applied

$$\beta_1 = 1 \text{ if } |m_1+m_2-m_3| = m_l, \text{ otherwise } 0 \quad (14a)$$

$$\beta_2 = 1 \text{ if } |m_2+m_3-m_1| = m_l, \text{ otherwise } 0 \quad (14b)$$

$$\beta_3 = 1 \text{ if } |m_3+m_1-m_2| = m_l, \text{ otherwise } 0 \quad (14c)$$

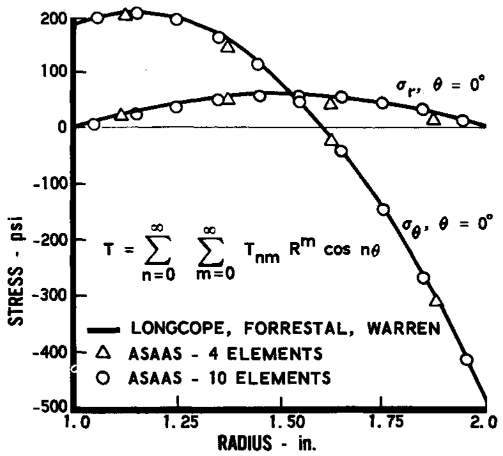

Fig. 2 Thermal stress in a transversely isotropic, hollow, circular cylinder.

$$\beta_4 = 1 \text{ if } |m_1+m_2+m_3| = m_l, \text{ otherwise } 0 \tag{14d}$$

The above is easily programed and is used to automatically derive the thermal stress.

The complete load vector for an element may now be found from the condition of orthogonality,

$$\{L\} = 2\pi[h]^T \left\{ \int \{[g_0]^T\{\tau_0\} + [e]^T\{F_0\}\} \, dr\, dz + \int [e]^T\{P_0\} ds \right\} + \pi \sum_{m_l=1}^{M_l} [h]^T \left\{ \int \{[g_{m_l}]^T\{\tau_{m_l}\} + [e]^T\{F_{m_l}\}\} \, dr\, dz + \int [e]^T\{P_{m_l}\} ds \right\}$$

where s is the arc length of the element on the surface of the solid and the matrix $[e]$ is given in the appendix.

Truncation of Fourier Series

In order to obtain a solution, it is necessary to truncate the Fourier series for displacements at some value, M_d. The Fourier series for loads and material properties are independent. However, the number of load harmonics, M_l, must be $\leq M_d$ in order to obtain a solution of the equation set. In general, as a result of circumferential variation of material properties, there is a coupling between all displacement harmonics and load harmonics. Therefore, displacement harmonics will exist that are not accounted for in the analysis. It is implicitly assumed that this coupling outside the range of M_d is insignificant due to rapid convergence of the Fourier series for displacement. For problems without sharp circumferential discontinuities, this assumption would appear to be justified. Also, the problems worked so far with the computer program tend to verify this conclusion.

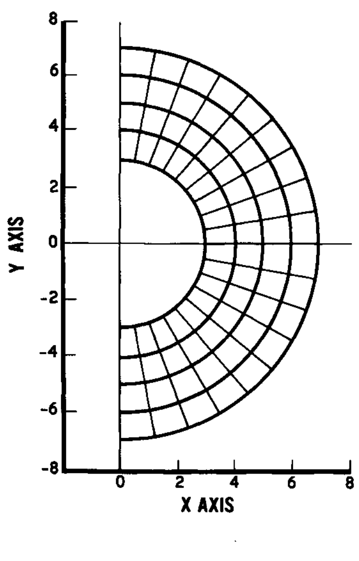

Fig. 3 Finite element grid for plane strain analysis.

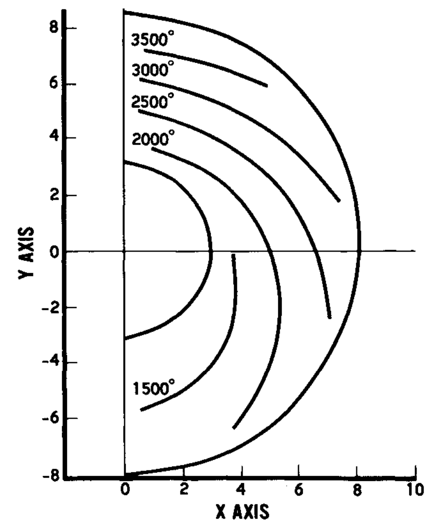

Fig. 4 Circumferential temperature distribution.

It can easily be seen that the stiffness matrix size increases as the square of the number of displacement harmonics. Therefore, for problems with detailed modeling in the meridional plane (200 or more quadrilateral elements), the number of harmonics is significantly limited by computer size. For this reason, the maximum number of harmonics allowed in the associated computer program was set equal to six. In addition, it would appear that when a problem requires more than six harmonics for adequate modeling, a three-dimensional finite element method[5] would be more efficient due to the total number of degrees of freedom involved.

ASAAS Computer Program

The ASAAS (Asymmetric Stress Analysis of Axisymmetric Solids) computer program was written for application of the method of analysis presented herein. The Fortran IV language was used and the program was structured to fit in five modules 69,120 single precision words) of an IBM 360, Model 65 MVT computer system. In order to have the capability of working problems large enough to be of practical value, considerable effort was expended to make the program compact and take advantage of the special characteristics of the method. With the program there is the capability of solving problems with up to 250 nodal points in the meridional plane and up to 6 terms in the Fourier series for displacements.

In order for the procedure to be feasible, it was necessary to apply a stiffness matrix bandwidth minimization procedure. In Ref. 6, it was shown that by ordering the terms of the displacement vector so that all the Fourier series components are lumped together for each meridional degree of freedom, a relatively narrow bandwidth can be achieved. For example, if a finite element gridwork has 9 nodal points in one direction and 27 in the other direction and 4 harmonics are used to idealize circumferential variations, the total number of equilibrium equations is 2916. The semibandwidth of this system is 132 terms if the procedures of Ref. 6 are followed. This gives rise to approximately 385,000 terms in the semiband of the symmetrical stiffness matrix. The problem is handled with a limited core storage by blocking and packing. That is, during generation of the stiffness matrix, storage is provided for only a few elements at a time and for only the nonzero terms of the stiffness matrix. In the preceding hypothetical problem, 8 elements would be processed during each block operation. This requires a core storage of less than the 20,000 locations available for the stiffness matrix. After each block of the stiffness matrix is computed, the block is output to an external storage device for use later in finding the solution.

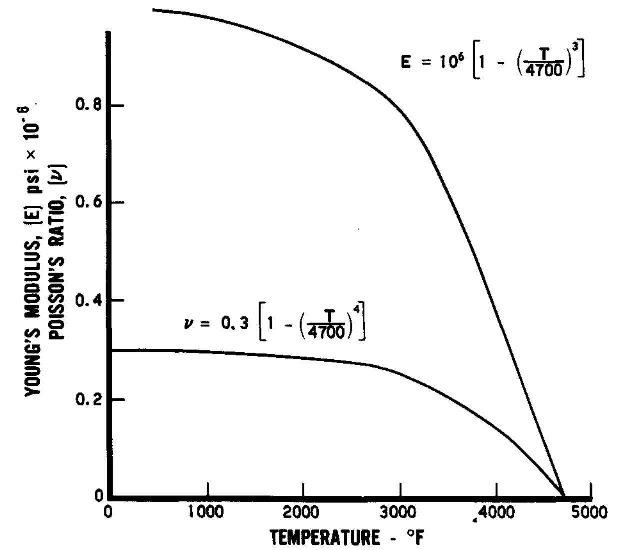

Fig. 5 Variation of elastic constants with temperature.

The solution of the equation set is obtained by a block modified square root Cholesky procedure. The equation set is blocked in such a way that the maximum available core storage (of 36,000 words) is used for each block. This is enough storage so that shifting of blocks in and out of core can be accomplished at logical steps of the factorization and forward and back substitutions. For example, in the above hypothetical problem, 132 columns can be factored with the data present in core before a block shift is necessary.

It was found that the limited accuracy of the IBM 360 single precision word leads to unacceptable roundoff errors in the solution of some problems. Therefore, an iterative refinement option[7] was added to the program. This option enables the program to yield accurate answers for all but the most ill-conditioned systems. For every six iterations, the time required for refinement is approximately equal to the time required to obtain the initial solution. In most cases, less than six iterations are required.

Element strains are computed from the resultant displacement solution by a finite-difference scheme.[8] This method has proved to be quite accurate and reduces the time for this step to a small fraction (5%) of the total job time. The alternative of recomputing element stiffness leads to prohibitive times because stiffness generation represents about 50% of total running time.

The total running time for the maximum size problem that the computer program is structured to solve is approximately 30 min on the Aerospace IBM 360/65 computer. Since the method is severely I/O bound, considerable opportunity exists for reducing the run time by utilizing high-speed drums (in place of the disk storage now used) and/or, more immediate access core storage.

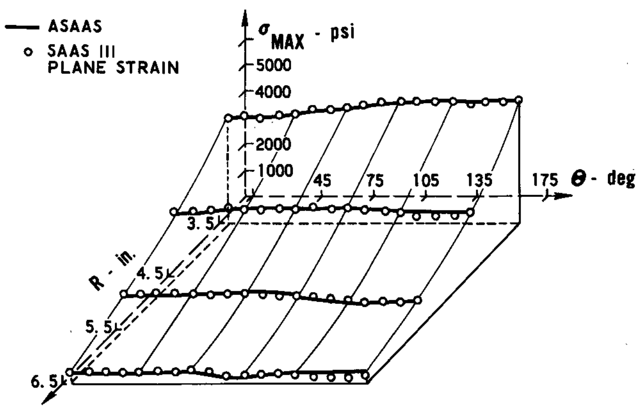

Fig. 6 Maximum thermal stress in infinite cylinder with temperature dependent properties.

Application

The computer program has been exercised on many problems. A few are presented here to demonstrate the accuracy, utility, and generality of the code. Input to the program is relatively simple. A two-dimensional automatic mesh generation procedure[2] allows easy meridional idealization of most structural configurations of interest. Only a few points on the perimeter of the solid are used to define the complete finite element gridwork. In addition, all Fourier coefficients of temperature and material properties are generated automatically within the code from point and tabular input. Output from the program can be printed and plotted. The printed output includes Fourier coefficients of the resultant displacement functions at each nodal point and total stresses and strains for each element at all desired circumferential locations. The plotted output consists of the meridional finite element grid and contours of stress, strain, or temperature plotted on meridional planes at any desired circumferential location.

Thermal Stresses in a Transversely Isotropic Hollow Circular Cylinder

An "exact" solution to the subject problem was developed in Ref. 9. Figure 2 shows the pertinent parameters along with part of the closed-form solution.[9] The problem was solved by the method presented herein and the results for a four element, two harmonic solution are represented by the triangles. A ten element solution, shown by circles, is much closer to the "exact" solution and serves to illustrate a high degree of accuracy for a relatively few number of elements and serves to verify that the method is convergent.

Plain Strain Analysis of Thermal Stress in a Hollow Circular Cylinder with Temperature Dependent Properties

In order to verify that the method of analysis is valid for problems where material properties vary circumferentially, a problem was formulated that could be solved by the present method and another generally accepted procedure. The subject problem was idealized in the cross section by a two-dimensional plane strain finite element computer program[2] with the mesh shown in Fig. 3. An asymmetric temperature field shown in Fig. 4 was input to the code along with the material property variation in Fig. 5. Then the same problem was solved by the present method with four elements in the meridional plane and three harmonics describing the circumferential variables. The maximum principal stress throughout the structure as calculated from both programs is plotted in Fig. 6. The excellent agreement obtained serves to verify that the circumferential material property variation is adequately modeled by the present method.

Thermal Stresses in a Spacecraft Heatshield

A quadrilateral finite element idealization of a spacecraft heatshield is shown in Fig. 7. Only half of the right circular cylindrical heatshield is modeled due to the symmetry of loading and geometry. Due to a mission abort, such a heatshield can

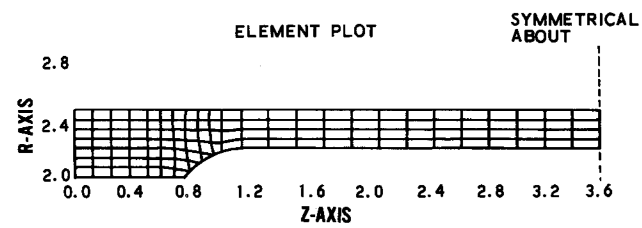

Fig. 7 Finite element idealization of spacecraft heatshield.

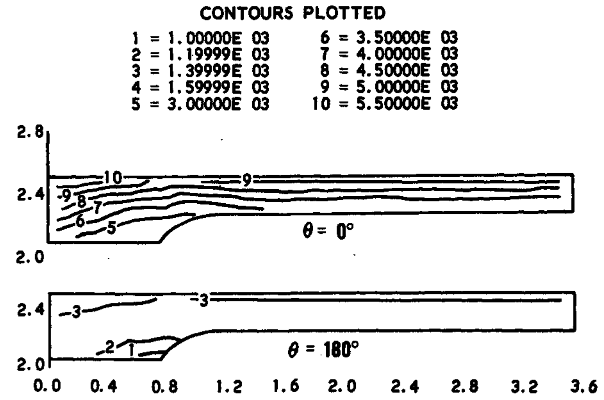

Fig. 8 Meridional temperature distribution.

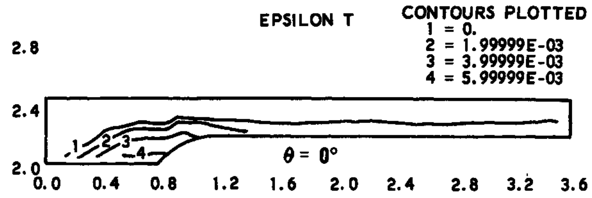

Fig. 9 Maximum principal strain in spacecraft heatshield.

be subjected to temperature variations as shown in Fig. 8. The results of applying the present method to this problem are shown in the form of a machine generated contour plot of maximum principal strain at $\theta = 0°$ in Fig. 9. This example problem illustrates the versatility of the method and its application to a fully three-dimensional problem. A total of 9 min was required on the Aerospace IBM 360 computer to solve this problem with three harmonics. The time included 3 iterations of the refinement option.

Summary

A method of analysis has been developed and forms the basis for a computer program (ASAAS) that can be successfully applied to the stress analysis of axisymmetric solids subjected to asymmetric mechanical and thermal loading and that provides the additional and unique capability of properly accounting for asymmetric material property variations. The resultant computer program has been made easy to use by incorporation of automatic mesh generation, Fourier coefficient generation, and contour plotting. The results have been verified by comparing solutions of simple problems with solutions obtained by other accepted methods.

Appendix

The following matrices are referred to in the text:

$$]_m] = \begin{bmatrix} \cos m\theta & 0 & 0 & 0 & 0 & 0 \\ 0 & \cos m\theta & 0 & 0 & 0 & 0 \\ 0 & 0 & \cos m\theta & 0 & 0 & 0 \\ 0 & 0 & 0 & \cos m\theta & 0 & 0 \\ 0 & 0 & 0 & 0 & \sin m\theta & 0 \\ 0 & 0 & 0 & 0 & 0 & \sin m\theta \end{bmatrix}$$

$$]_m] = \begin{bmatrix} 0 & 1 & 0 & 0 & 0 & 0 & 0 & 0 & 0 \\ 0 & 0 & 0 & 0 & 0 & 1 & 0 & 0 & 0 \\ \frac{1}{r} & 1 & \frac{z}{r} & 0 & 0 & 0 & \frac{m}{r} & m & \frac{mz}{r} \\ 0 & 0 & 1 & 0 & 1 & 0 & 0 & 0 & 0 \\ -\frac{m}{r} & -m & -\frac{zm}{r} & 0 & 0 & 0 & -\frac{1}{r} & 0 & -\frac{z}{r} \\ 0 & 0 & 0 & -\frac{m}{r} & -m & -\frac{zm}{r} & 0 & 0 & 1 \end{bmatrix}$$

$$[e] = \begin{bmatrix} 1 & r & z & 0 & 0 & 0 & 0 & 0 & 0 \\ 0 & 0 & 0 & 1 & r & z & 0 & 0 & 0 \\ 0 & 0 & 0 & 0 & 0 & 0 & 1 & r & z \end{bmatrix}$$

$$[h] = \frac{1}{\lambda}\begin{bmatrix} h_{11} & 0 & 0 & h_{12} & 0 & 0 & h_{13} & 0 & 0 \\ h_{21} & 0 & 0 & h_{22} & 0 & 0 & h_{23} & 0 & 0 \\ h_{31} & 0 & 0 & h_{32} & 0 & 0 & h_{33} & 0 & 0 \\ 0 & h_{11} & 0 & 0 & h_{12} & 0 & 0 & h_{13} & 0 \\ 0 & h_{21} & 0 & 0 & h_{22} & 0 & 0 & h_{23} & 0 \\ 0 & h_{31} & 0 & 0 & h_{32} & 0 & 0 & h_{33} & 0 \\ 0 & 0 & h_{11} & 0 & 0 & h_{12} & 0 & 0 & h_{13} \\ 0 & 0 & h_{21} & 0 & 0 & h_{22} & 0 & 0 & h_{23} \\ 0 & 0 & h_{31} & 0 & 0 & h_{32} & 0 & 0 & h_{33} \end{bmatrix}$$

where

$$\lambda = r_j(z_k - z_i) + r_i(z_j - z_k) + r_k(z_i - z_j)$$

$$h_{11} = r_j z_k - r_k z_j, \quad h_{12} = r_k z_i - r_i z_k, \quad h_{13} = r_i z_j - r_j z_i$$
$$h_{21} = z_j - z_k, \quad h_{22} = z_k - z_i, \quad h_{23} = z_i - z_j$$
$$h_{31} = r_k - r_j, \quad h_{32} = r_i - r_k, \quad h_{33} = r_j - r_i$$

and the subscripts i, j, k refer to the three nodal points of the triangular ring element proceeding counterclockwise in a right-handed $r-z$ coordinate system

$$[C_{m_m}] = [A_m]$$

where

$$[A_m] = \begin{bmatrix} a_{11m} & a_{12m} & a_{13m} & a_{14m} & 0 & 0 \\ a_{21m} & a_{22m} & a_{23m} & a_{24m} & 0 & 0 \\ a_{31m} & a_{32m} & a_{33m} & a_{34m} & 0 & 0 \\ a_{41m} & a_{42m} & a_{43m} & a_{44m} & 0 & 0 \\ 0 & 0 & 0 & 0 & a_{55m} & a_{56m} \\ 0 & 0 & 0 & 0 & a_{65m} & a_{66m} \end{bmatrix}$$

and where for transverse isotropy

$$[A_m] = \begin{bmatrix} \left(\frac{1}{E_r}\right)_{m_m} & \left(-\frac{v_{rz}}{E_r}\right)_{m_m} & \left(-\frac{v_{r\theta}}{E_r}\right)_{m_m} & 0 & 0 & 0 \\ \left(-\frac{v_{rz}}{E_r}\right)_{m_m} & \left(\frac{1}{E_z}\right)_{m_m} & \left(-\frac{v_{z\theta}}{E_z}\right)_{m_m} & 0 & 0 & 0 \\ \left(-\frac{v_{r\theta}}{E_r}\right)_{m_m} & \left(-\frac{v_{z\theta}}{E_z}\right)_{m_m} & \left(\frac{1}{E_\theta}\right)_{m_m} & 0 & 0 & 0 \\ 0 & 0 & 0 & \left(\frac{1}{G_{rz}}\right)_{m_m} & 0 & 0 \\ 0 & 0 & 0 & 0 & \left(\frac{1}{G_{r\theta}}\right)_{m_m} & 0 \\ 0 & 0 & 0 & 0 & 0 & \left(\frac{1}{G_{z\theta}}\right)_{m_m} \end{bmatrix}^{-1}$$

E is Young's modulus, v is Poisson's ratio, and G is the shear modulus. Poisson's ratio is defined as

$$v_{ij} = -\varepsilon_j/\varepsilon_i \quad \text{for the uniaxial loading} \quad \sigma_i = \sigma$$

In the associated computer program, the principal axes of the orthotropic material need not be aligned with r and z. Therefore, other terms appear in $[A]$ as indicated by the presence of nonzero terms not defined previously. The appropriate transformation is used to rotate the preceding matrix in that case

$$[\phi_{m_i,m_d}] = [\phi]$$

where

$\phi_{11} = (C_{33}+m_l m_d C_{55})\int (1/r^2)\,dr\,dz$

$\phi_{12} = (C_{31}+C_{33}+m_l m_d C_{55})\int (1/r)\,dr\,dz$

$\phi_{13} = C_{34}\int (1/r)\,dr\,dz+(C_{33}+m_l m_d C_{55})\int (z/r^2)\,dr\,dz$

$\phi_{14} = m_l m_d C_{56}\int (1/r^2)\,dr\,dz$

$\phi_{15} = (C_{34}+m_l m_d C_{56})\int (1/r)\,dr\,dz$

$\phi_{16} = C_{32}\int (1/r)\,dr+m_l m_d C_{56}\int (z/r^2)\,dr\,dz$

$\phi_{17} = (m_l C_{33}+m_d C_{55})\int (1/r^2)\,dr\,dz;\quad \phi_{18} = m_l C_{33}\int (1/r)\,dr\,dz$

$\phi_{19} = (m_l C_{33}+m_d C_{55}\int (z/r^2)\,dr\,dz-m_d C_{56}\int (1/r)\,dr\,dz$

$\phi_{21} = \phi_{12};\quad \phi_{22} = (C_{11}+2C_{13}+C_{33}+m_l m_d C_{55})\int dr\,dz$

$\phi_{23} = (C_{13}+C_{33}+m_l m_d C_{55})\int (z/r)\,dr\,dz+(C_{14}+C_{34})\int dr\,dz$

$\phi_{24} = m_l m_d C_{56}\int (1/r)\,dr\,dz$

$\phi_{25} = (C_{14}+C_{34}+m_l m_d C_{56})\int dr\,dz$

$\phi_{26} = (C_{12}+C_{23})\int dr\,dz+m_l m_d C_{56}\int (z/r)\,dr\,dz$

$\phi_{27} = [m_d(C_{13}+C_{33})+m_l C_{55}]\int (1/r)\,dr\,dz$

$\phi_{28} = m_d(C_{13}+C_{33})\int dr\,dz$

$\phi_{29} = [m_d(C_{13}+C_{33})+m_l C_{55}]\int (z/r)\,dr\,dz-m_l C_{56}\int dr\,dz$

$\phi_{31} = \phi_{13};\quad \phi_{32} = \phi_{23}$

$\phi_{33} = (C_{33}+m_l m_d C_{55})\int (z^2/r^2)\,dr\,dz+2C_{34}\int (z/r)\,dr\,dz+ C_{44}\int dr\,dz$

$\phi_{34} = m_l m_d C_{56}\int (z/r^2)\,dr\,dz$

$\phi_{35} = (C_{34}+m_l m_d C_{56})\int (z/r)\,dr\,dz+C_{44}\int dr\,dz$

$\phi_{36} = C_{23}\int (z/r)\,dr\,dz+C_{24}\int dr\,dz+m_l m_d C_{56}\int (z^2/r^2)\,dr\,dz$

$\phi_{37} = (m_d C_{33}+m_l C_{55})\int (z/r^2)\,dr\,dz+m_d C_{34}\int (1/r)\,dr\,dz$

$\phi_{38} = m_d C_{33}\int (z/r)\,dr\,dz+m_d C_{34}\int dr\,dz$

$\phi_{39} = (m_d C_{33}+m_l C_{55})\int (z^2/r^2)\,dr\,dz+ (m_d C_{34}-m_l C_{56})\int (z/r)\,dr\,dz$

$\phi_{41} = \phi_{14};\quad \phi_{42} = \phi_{24};\quad \phi_{43} = \phi_{34}$

$\phi_{44} = m_l m_d C_{66}\int (1/r_2)\,dr\,dz;\quad \phi_{45} = m_l m_d C_{66}\int (1/r)\,dr\,dz$

$\phi_{46} = m_l m_d C_{66}\int (z/r^2)\,dr\,dz;\quad \phi_{47} = m_l C_{56}\int (1/r^2)\,dr\,dz$

$\phi_{48} = 0;\quad \phi_{49} = m_l C_{56}\int (z/r^2)\,dr\,dz-m_l C_{66}\int (1/r)\,dr\,dz$

$\phi_{51} = \phi_{15};\quad \phi_{52} = \phi_{25};\quad \phi_{53} = \phi_{35};\quad \phi_{54} = \phi_{45}$

$\phi_{55} = (C_{44}+m_l m_d C_{66})\int dr\,dz$

$\phi_{56} = C_{24}\int dr\,dz+m_l m_d C_{66}\int (z/r)\,dr\,dz$

$\phi_{57} = (m_d C_{34}+m_l C_{56})\int (1/r)\,dr\,dz;\quad \phi_{58} = m_d C_{34}\int dr\,dz$

$\phi_{59} = (m_d C_{34}+m_l C_{56})\int (z/r)\,dr\,dz-m_l C_{66}\int dr\,dz$

$\phi_{61} = \phi_{16};\quad \phi_{62} = \phi_{26};\quad \phi_{63} = \phi_{36};\quad \phi_{64} = \phi_{46};\quad \phi_{65} = \phi_{56}$

$\phi_{66} = C_{22}\int dr\,dz+m_l m_d C_{66}\int (z^2/r^2)\,dr\,dz$

$\phi_{67} = m_d C_{23}\int (1/r)\,dr\,dz+m_l C_{56}\int (z^2/r^2)\,dr\,dz$

$\phi_{68} = m_d C_{23}\int dr\,dz$

$\phi_{69} = m_l C_{56}\int (z^2/r^2)\,dr\,dz+(m_d C_{23}-m_l C_{66})\int (z/r)\,dr\,dz$

$\phi_{71} = (m_l C_{33}+m_d C_{55})\int (1/r^2)\,dr\,dz$

$\phi_{72} = [m_l(C_{13}+C_{33})+m_d C_{55}]\int (1/r)\,dr\,dz$

$\phi_{73} = (m_l C_{33}+m_d C_{55})\int (z/r^2)\,dr\,dz+m_l C_{34}\int (1/r)\,dr\,dz$

$\phi_{74} = m_d C_{56}\int (1/r^2)\,dr\,dz$

$\phi_{75} = (m_l C_{34}+m_d C_{56})\int (1/r)\,dr\,dz$

$\phi_{76} = m_l C_{23}\int (1/r)\,dr\,dz+m_d C_{56}\int (z/r^2)\,dr\,dz$

$\phi_{77} = (m_l m_d C_{33}+C_{55})\int (1/r^2)\,dr\,dz$

$\phi_{78} = m_l m_d C_{33}\int (1/r)\,dr\,dz$

$\phi_{79} = (m_l m_d C_{33}+C_{55})\int (z/r^2)\,dr\,dz-C_{56}\int (1/r)\,dr\,dz$

$\phi_{81} = m_l C_{33}\int (1/r)\,dr\,dz;\quad \phi_{82} = m_l(C_{13}+C_{33})\int dr\,dz$

$\phi_{83} = m_l C_{33}\int (z/r)\,dr\,dz+m_l C_{34}\int dr\,dz$

$\phi_{84} = 0;\quad \phi_{85} = m_l C_{34}\int dr\,dz;\quad \phi_{86} = m_l C_{23}\int dr\,dz$

$\phi_{87} = \phi_{78};\quad \phi_{88} = m_l m_d C_{33}\int dr\,dz;\quad \phi_{89} = m_l m_d C_{33}\int (z/r)\,dr\,dz$

$\phi_{91} = (m_l C_{33}+m_d C_{55})\int (z/r^2)\,dr\,dz-m_d C_{56}\int (1/r)\,dr\,dz$

$\phi_{92} = [m_l(C_{13}+C_{33})+m_d C_{55}]\int (z/r)\,dr\,dz-m_d C_{56}\int dr\,dz$

$\phi_{93} = (m_l C_{33}+m_d C_{55})\int (z^2/r^2)\,dr\,dz+ (m_l C_{34}-m_d C_{56})\int (z/r)\,dr\,dz$

$\phi_{94} = m_d C_{56}\int (z/r^2)\,dr\,dz-m_d C_{66}\int (1/r)\,dr\,dz$

$\phi_{95} = (m_l C_{34}+m_d C_{56})\int (z/r)\,dr\,dz-m_d C_{66}\int dr\,dz$

$\phi_{96} = m_d C_{56}\int (z^2/r^2)\,dr\,dz+(m_l C_{23}-m_d C_{66})\int (z/r)\,dr\,dz$

$\phi_{97} = \phi_{79};\quad \phi_{98} = \phi_{89}$

$\phi_{99} = (m_l m_d C_{33}+C_{55})\int (z^2/r^2)\,dr\,dz- 2C_{56}\int (z/r)\,dr\,dz+C_{66}\int dr\,dz$

where

$$C_{ij} = \sum_{m_m=0}^{M_m} a_{ijm_m}\int_0^{2\pi} \cos m_l\theta \cos m_m\theta \cos m_d\theta\, d\theta \quad \begin{cases} i<5 \\ j<5 \end{cases}$$

$$C_{ij} = \sum_{m_m=0}^{M_m} a_{ijm_m}\int_0^{2\pi} \sin m_l\theta \cos m_m\theta \sin m_d\theta\, d\theta \quad \begin{cases} i>4 \\ j>4 \end{cases}$$

Performing the integrations results in the following rule for combining material harmonics in the element stiffness matrix

$$C_{ij} = (\pi/2)(a_{ij(m_l+m_d)}+a_{ij(|m_l-m_d|)}+\gamma_1 a_{ij0}+\gamma_2 a_{ij0}) \quad \text{for } i<5, j<5$$

$$C_{ij} = (\pi/2)[(1-\gamma_2)a_{ij(|m_l-m_d|)}-a_{ij(m_l+m_d)}+\gamma_1 a_{ij0}] \quad \text{for } i>4, j>4$$

$$\gamma_1 = 0 \text{ if } m_l \neq m_d,\quad \gamma_1 = 1 \text{ if } m_l = m_d$$

$$\gamma_2 = 0 \text{ if } m_l \neq 0 \text{ or } m_d \neq 0,\quad \gamma_2 = 1 \text{ if } m_l = m_d = 0$$

References

[1] Wilson, E. L., "Structural Analysis of Axisymmetric Solids," *AIAA Journal,* Vol. 3, No. 12, Dec. 1965, pp. 2269–2274.

[2] Crose, J. G. and Jones, R. M., "SAAS III, Finite Element Stress Analysis of Axisymmetric and Plane Solids with Different Orthotropic, Temperature Dependent Material Properties in Tension and Compression," TR-0059(S6816-53)-1, June 1971, The Aerospace Corp., San Bernardino, Calif.

[3] Brisbane, J. J., "Finite Element Stress Analysis of Anistropic Bodies," Rept. S-143, Aug. 1968, Rohn & Haas, Huntsville, Ala.

[4] Dunham, R. S. and Nickell, R. E., "Finite Element Analysis of Axisymmetric Solids with Arbitrary Loadings," Structural Engineering Lab. Rept. 67–6, June 1967, Univ. of California, Berkeley, Calif.

[5] Argyris, J. H., Buck, K. E., Grieger, I., and Mareczek, G., "Application of the Matrix Displacement Method to the Analysis of Pressure Vessels," *Transactions of the ASME,* Vol. 92, Ser. B, May 2, 1970, pp. 317–329.

[6] Crose, J. G., "Bandwidth Minimization of Stiffness Matrices," *Journal of the Engineering Mechanics Division,* ASCE, EM1, Feb. 1971, pp. 163–167.

[7] Martin, R. S., Peters, G., and Wilkinson, J. H., "Iterative Refinement of the Solution of a Positive Definite System of Equations," *Numerische Mathematik,* Vol. 8, 1966, pp. 203–216.

[8] Galloway, J. C. and Ang, A. H.-S., "A Generalized Lumped-Parameter Model for Plane Problems of Solid Media," Structural Research Ser. 341, Nov. 1968, Univ. of Illinois, Urbana, Ill.

[9] Longcope, D. B., Forrestal, M. J., and Warren, W. E., "Thermal Stresses in a Transversely Isotropic, Hollow, Circular Cylinder," *AIAA Journal,* Vol. 7, No. 11, Nov. 1969, pp. 2174–2176.